The Astrophysical Journal, 638:1169–1175, 2006 February 20

THE NEARLY ISOTROPIC VELOCITY DISTRIBUTIONS OF ENERGETIC ELECTRONS IN THE SOLAR WIND

Q. M. Lu,[1] C. S. Wu,[1,2] and S. Wang[1]
Received 2005 February 27; accepted 2005 October 14

ABSTRACT

Observations with *Wind* and other spacecraft of the solar wind have shown that the velocity distributions of energetic electrons associated with solar impulsive electron events are often nearly isotropic, as shown by Lin et al. and Ergun et al. It is believed that in each case the electrons are originally associated with a flare-associated beam. The issue of interest is: how can a beam of fast electrons evolve into such a final state? This paper offers a theoretical explanation. We attribute the isotropization of the electron beam distribution to nonresonant pitch-angle scattering by enhanced Alfvén waves in the corona and the solar wind. The proposed scenario is demonstrated with test particle calculations.

Subject heading: solar wind

1. INTRODUCTION

The velocity distribution function of an electron beam associated with solar impulsive electron events measured with the *Wind* 3-D Plasma and Energetic Particles instrument in the solar wind is reported in Lin et al. (1996) and Ergun et al. (1998), and the results show that the velocity distributions of energetic electrons often appear nearly isotropic in the solar wind (see Fig. 1, a contour plot of the two-dimensional electron distribution). It is strongly believed that in each case these energetic electrons are originally associated with a flare-associated electron beam, as evidenced by a weak beam feature that is often visible, and by correlative study of observed flare events. Similar results were observed previously with other spacecraft (Lin et al. 1981, 1986, 1995).

The above-mentioned observational results raise two important questions: (1) what process can make an initial beam distribution evolve into the nearly isotropic velocity distribution, and (2) what is the meaning of those energetic electrons with a sunward velocity component along the ambient magnetic field?

The first question is intriguing because the usual quasi-linear relaxation due to enhanced Langmuir waves, as discussed in Grognard (1985), Melrose & Goldman (1987), and Muschietti (1990), cannot resolve the issue. Here, we suggest that enhanced Alfvénic turbulence in the corona and the solar wind (e.g., Belcher 1971; Jacques 1977; Pijpers 1995; Ofman & Davila 1997; Tu & Marsch 1997) may play a pivotal role since these waves pervade interplanetary space. Our contention is that the intrinsic Alfvén waves are responsible for the observed distribution function. Admittedly, such a scenario may not be in line with the familiar concept derived from linear kinetic theory that electrons cannot interact with Alfvén wave via cyclotron resonance because

$$k|v_{\|} - V_{\rm A}| \ll |\Omega_e|, \qquad (1)$$

where k is the wavenumber of the Alfvén waves, $V_{\rm A}$ is the Alfvén speed, $v_{\|}$ is the particle velocity in the direction of the ambient magnetic field, and Ω_e is the electron cyclotron frequency. The point, which we want to advocate, is that electrons can interact with Alfvén waves with finite amplitude without recourse to cyclotron resonance. In order to clarify this point, a discussion along this line is presented in this paper.

The paper is organized as follows. In § 2, we describe the theoretical model used to illustrate the interaction between intrinsic Alfvén waves and electrons. Test particle calculations for the evolution of the electron beam distribution in the presence of Alfvén waves are presented in § 3. The discussion and conclusions are given in § 4, as are the comparisons with the *Wind* spacecraft observations.

2. ELECTRON-ALFVÉN WAVE INTERACTIONS: ANALYTIC STUDY

Linearized Vlasov theory leads many people to believe that electrons cannot interact with Alfvén waves. This belief stems from the notion that electrons cannot satisfy the cyclotron resonance condition because the electron cyclotron frequency is too high. However, the above conclusion is true only when the wave amplitude is exceedingly small. We must point out that Alfvén waves with finite amplitudes can interact with electrons without recourse to cyclotron resonance. To clarify this point, a discussion of the basic interaction process is pertinent.

We remark at the outset that in general there are two types of wave-particle interaction processes, resonant and nonresonant. For instance, energetic protons may interact with Alfvén waves via cyclotron resonance, but for slow ions nonresonant interactions prevail. Here we also want to remark that nonresonant interaction is far more efficient, provided that the wave energy density is sufficiently high. The primary reason is that in general the resonant interaction process only involves one Fourier wave component while the nonresonant interaction process involves the entire wave field.

For electrons, the possibility of nonresonant interaction with Alfvén waves is usually overlooked. In the following we focus our discussion on this process. In fact we show that Alfvén waves can interact with protons and electrons equally efficiently under the nonresonant process.

To proceed with the discussion, let us consider the situation in which intrinsic Alfvén waves are propagating along the ambient magnetic field $\boldsymbol{B}_0$, which is parallel to the z-axis. In the following we denote the wave magnetic field by $\delta\boldsymbol{B}_w$ and the wave electric field by $\delta\boldsymbol{E}_w$. They are both perpendicular to the ambient magnetic field and may be expressed as

$$\delta\boldsymbol{E}_w = -\frac{v_A}{c}\boldsymbol{b}\times\delta\boldsymbol{B}_w, \qquad (2)$$

[1] School of Earth and Space Sciences, University of Science and Technology of China, Hefei, Anhui 230026, China.
[2] Institute for Physical Science and Technology, University of Maryland, College Park, MD 20742.

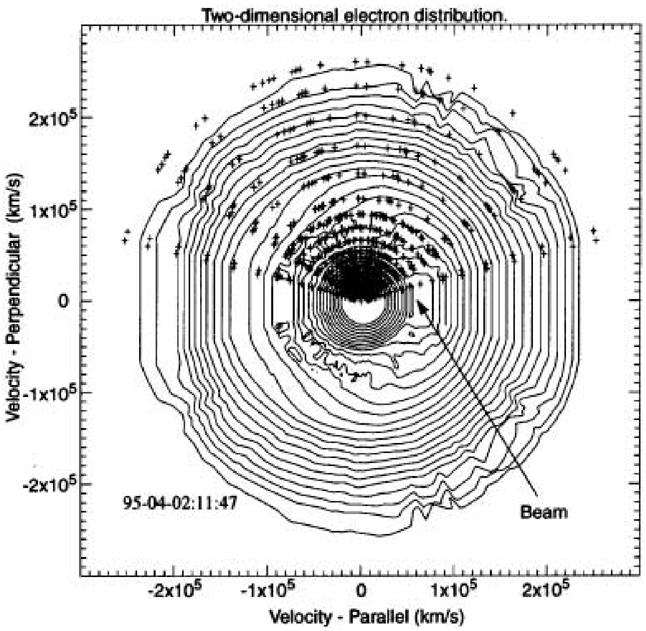

FIG. 1.—Contour plot of the two-dimensional electron distribution, which includes the beam and background electrons. The contours represent logarithmically spaced levels. The plus signs are the center velocities of the EESAH and SST Foil detectors. The beam is at $\sim 6\times10^4$ km s^{-1}. (After Ergun et al. 1998.)

where $\boldsymbol{b} = \boldsymbol{B}_0/B_0$ and $v_{\rm A}$ is the Alfvén speed. Hereafter we consider that the waves are circularly polarized so that

$$\delta\boldsymbol{B}_w = \sum_k B_k^{\pm}\left[\cos\phi_k^{\pm}\boldsymbol{i}_x \pm \sin\phi_k^{\pm}\boldsymbol{i}_y\right], \qquad (3)$$

where $\boldsymbol{i}_x$ and $\boldsymbol{i}_y$ are unit directional vectors, $\pm$ indicates that either the waves are right-hand polarized or left-hand polarized, $\phi_k^{\pm}$ denotes the wave phase

$$\phi_k^{\pm} = k(v_{\rm A}t - z) + \varphi_k^{\pm}, \qquad (4)$$

and $\varphi_k^{\pm}$ is a phase constant. It is convenient to write the equations of motion in terms of the following quantities, as considered in Wu et al. (1997),

$$u_\perp = v_x + iv_y, \qquad (5)$$

$$\delta B_w = \sum_k B_k e^{\pm i\phi_k^{\pm}}, \qquad (6)$$

so that

$$\frac{du_\perp}{dt} + i\Omega_{\alpha0}u_\perp = i(v_\parallel - v_{\rm A})\sum_k \Omega_{\alpha k}e^{\pm i\phi_k^{\pm}}, \qquad (7)$$

$$\frac{dv_\parallel}{dt} = -{\rm Im}\left(u_\perp \sum_k \Omega_{\alpha k}e^{\pm i\phi_k^{\pm}}\right), \qquad (8)$$

$$\frac{dz}{dt} = v_\parallel. \qquad (9)$$

In the above equations we have defined $\Omega_{\alpha0} = e_\alpha B_0/m_\alpha c$, $\Omega_{\alpha k} = e_\alpha B_k/m_\alpha c$, and the subscript α to indicate physical quantities associated with particles of species α. In the present discussion we use Gaussian units.

We look for the solutions of the above equations with the initial conditions at $t = 0$, $v_\parallel = v_\parallel(0)$, $u_\perp = u_\perp(0)$, and $z = z(0)$. Hereafter, we consider that $\Omega_{\alpha k}/\Omega_{\alpha0} = B_k/B_0 \ll 1$ and $|\Omega_{\alpha0}| \gg \left|k[v_\parallel(0) - v_{\rm A}]\right|$. In view of equation (8) we assume that quantities on the right-hand side of equation (7) vary only slightly during a cyclotron period so that they may be approximated by the initial values. Considering the random-phase approximation, we obtain

$$u_\perp(t)e^{i\Omega_{\alpha0}t} = u_\perp(0) - \left[v_{\rm A} - v_\parallel(0)\right]\sum_k \frac{e_\alpha B_k}{m_\alpha c}e^{\pm i[\phi_k - kz(0)]}\left(\frac{e^{i\left\{\Omega_{\alpha0}\pm k\left[v_{\rm A}-v_\parallel(0)\right]\right\}t} - 1}{\Omega_{\alpha0} \pm k[v_{\rm A} - v_\parallel(0)]}\right), \qquad (10)$$

$$\begin{aligned} v_\parallel(t) = v_\parallel(0) - \Bigg(&\sum_k v_\perp(0)\frac{e_\alpha B_k}{m_\alpha c}\cos\Phi_k(0) \\ &- \sum_k \frac{\left[v_\parallel(0) - v_{\rm A}\right]}{\left\{\Omega_{\alpha0} \pm k\left[v_\parallel(0) - v_{\rm A}\right]\right\}}\frac{e_\alpha^2 B_k^2}{m_\alpha^2 c^2}\Bigg) \\ &\times \frac{\left(\cos\left\{\Omega_{\alpha0} \pm k\left[v_{\rm A} - v_\parallel(0)\right]\right\}t - 1\right)}{\left(\Omega_{\alpha0} \pm k\left[v_{\rm A} - v_\parallel(0)\right]\right)} \\ &+ \sum_k v_\perp(0)\frac{e_\alpha B_k}{m_\alpha c}\sin\Phi_k(0)\frac{\sin\left\{\Omega_{\alpha0} \pm k\left[v_{\rm A} - v_\parallel(0)\right]\right\}t}{\left\{\Omega_{\alpha0} \pm k\left[v_{\rm A} - v_\parallel(0)\right]\right\}}, \end{aligned} \qquad (11)$$

where

$$\Phi_k = \theta(0) \mp [\varphi_k^{\pm} - kz(0)]$$

and $\theta(0)$ is the gyro–phase angle of a particle at $t = 0$. Evidently the solutions look complicated. In order to extract the essence of the physics from the above results, let us consider the special case in which $v_\perp(0) \ll \left|v_\parallel(0) - v_{\rm A}\right|$ so that equation (11) reduces to

$$v_\parallel(t) = v_\parallel(0) + \left\{\sum_k \left[v_\parallel(0) - v_{\rm A}\right]\frac{e_\alpha^2 B_k^2}{m_\alpha^2 c^2}\right\}\frac{\left(\cos\left\{\Omega_{\alpha0} \pm k\left[v_{\rm A} - v_\parallel(0)\right]\right\}t - 1\right)}{\left\{\Omega_{\alpha0} \pm k\left[v_{\rm A} - v_\parallel(0)\right]\right\}^2}. \qquad (12)$$

Since $|\Omega_{\alpha0}| \gg \left|k[v_\parallel(0) - v_{\rm A}]\right|$ is true for particles of interest, equation (12) yields

$$v_\parallel(t) = v_\parallel(0) + \sum_k \frac{B_k^2}{B_0^2}\left[v_\parallel(0) - v_{\rm A}\right](\cos\Omega_{\alpha0}t - 1). \qquad (13)$$

From equation (13) we see that $v_\parallel$ is modified by the intrinsic Alfvén waves. The amount

$$\begin{aligned}\Delta v_\parallel(t) &= \sum_k \frac{B_k^2}{B_0^2}\left[v_\parallel(0) - v_{\rm A}\right](\cos\Omega_{\alpha0}t - 1) \\ &= \frac{\delta B_w^2}{B_0^2}\left[v_\parallel(0) - v_{\rm A}\right](\cos\Omega_{\alpha0}t - 1)\end{aligned}$$

oscillates with time. There are two important points: one is that the magnitude does not depend on particle species, although the

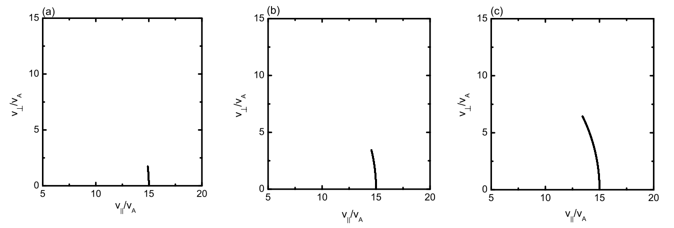

FIG. 2.—Time evolution of the electron velocity components $v_\parallel$ and $v_\perp$ (the subscripts $\parallel$ and $\perp$ denote the direction parallel and perpendicular to the ambient magnetic field, respectively) for three cases: (*a*) $\delta B_w^2/B_0^2 = 0.004$, (*b*) $\delta B_w^2/B_0^2 = 0.016$, and (*c*) $\delta B_w^2/B_0^2 = 0.064$. The results are based on eq. (13) in the theoretical model.

time period does, and the other is that the entire spectrum of the wave affects the motion of the particle.

In conclusion, when nonresonant interactions dominate, Alfvén waves can influence electrons just as effectively as they act on ions. Hereafter we focus our attention on electrons. For illustration purposes in Figure 2 we depict the time evolution of electron velocity components $v_\parallel$ and $v_\perp$ for three cases: (*a*) $\delta B_w^2/B_0^2 = 0.004$, (*b*) $\delta B_w^2/B_0^2 = 0.016$, and (*c*) $\delta B_w^2/B_0^2 = 0.064$. The electron velocity is initially set as $(v_\parallel, v_\perp) = (15v_A, 0)$. The parallel velocities are calculated according to equation (13). The numerical results are obtained by iteration. The scheme is first to calculate $v_\parallel$ and then to compute $v_\perp$ based on the fact that

$$\left(v_\parallel - v_A\right)^2 + v_\perp^2 = \text{constant}. \qquad (14)$$

Electrons move on the spherical surface in velocity space defined by equation (14). When the amplitude of the enhanced Alfvén waves is increased, the range of the electron pitch angles on the spherical surface also increases. Obviously, the electrons can interact with the enhanced Alfvén waves without relying on the resonance condition. However, when the amplitude of the enhanced Alfvén waves is sufficiently large and comparable to the ambient magnetic field, the existence conditions for equation (13) are not satisfied. To discuss the time evolution of the velocity distribution in such cases, test particle calculations are necessary.

3. ELECTRON-ALFVÉN WAVE INTERACTIONS: NUMERICAL CALCULATIONS

It is well discussed in the literature that fast ions can be pitch-angle scattered (Winske et al. 1985; Yoon & Wu 1991; Onsager et al. 1991; Akimoto et al. 1993; Daughton et al. 1999) and that slow ions can be heated by Alfvén waves (Li et al. 1997; Chen et al. 2001). In both cases nonresonant interactions play primary roles. Based on the study discussed in § 2, we see that Alfvén waves can also pitch-angle scatter fast electrons via nonresonant interactions if electrons have velocities sufficiently higher than the Alfvén speed. In order to demonstrate this point we carry out numerical calculations, which are discussed below.

The principal task of our calculation is to study the motion of a beam of fast electrons under the influence of intrinsic Alfvén waves. The method used is a series of test particle calculations in which we only consider the influence of the wave fields on the motions of the electrons while the effects of the electrons on the waves are neglected. In the calculation, the ratio of the proton to electron mass is taken to be $m_p/m_e = 1836$, where the subscripts *p* and *e* denote proton and electron species, respectively. The speed of light is $c = 150v_A$. Initially, the electron beam flows in the +*z*-direction. If not stated explicitly, the bulk velocity of the

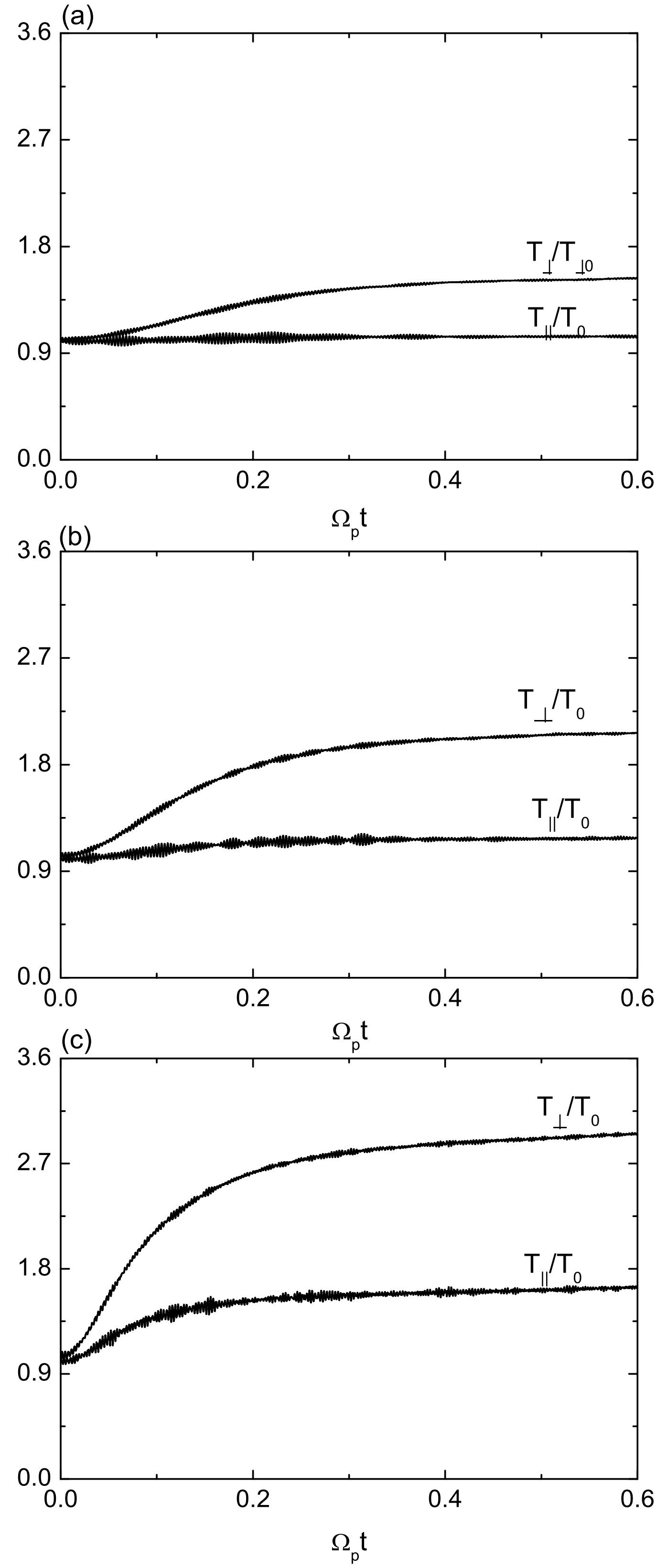

FIG. 3.—Time evolution of the effective parallel and perpendicular temperature $T_\parallel/T_0$ and $T_\perp/T_0$, respectively, for three cases: (*a*) $\delta B_w^2/B_0^2 = 0.064$, (*b*) $\delta B_w^2/B_0^2 = 0.142$, and (*c*) $\delta B_w^2/B_0^2 = 0.319$. The results are based on test particle calculations.

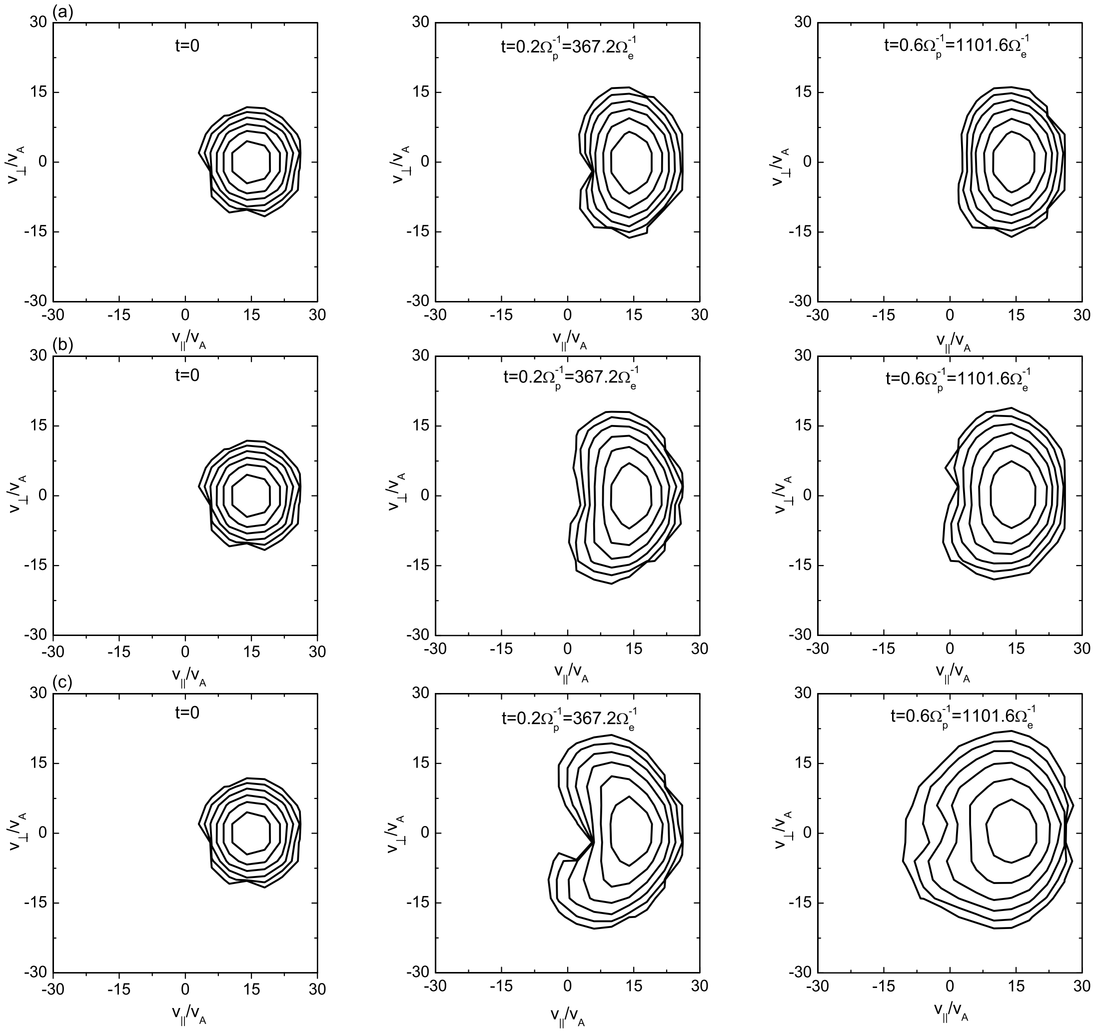

FIG. 4.—Contour plots of the velocity distribution function of the electron beam at $t = 0$, $0.2\Omega_p^{-1}$, and $0.6\Omega_p^{-1}$ for three cases: (*a*) $\delta B_w^2/B_0^2 = 0.064$, (*b*) $\delta B_w^2/B_0^2 = 0.142$, and (*c*) $\delta B_w^2/B_0^2 = 0.319$, where $v_\perp = (v_x^2 + v_y^2)^{1/2}$. The top half of each panel corresponds to $v_y > 0$, while the bottom half corresponds to $v_y < 0$. The contours represent logarithmically spaced levels. The results are based on test particle calculations.

electron beam $u_b = 15v_A$, and the velocity dispersion is $v_{the} = 3.0v_A$. The electron dynamics are described by

$$m_e \frac{d\boldsymbol{v}}{dt} = -e\left[\delta\boldsymbol{E}_w + \frac{\boldsymbol{v}}{c} \times (B_0\boldsymbol{i}_z + \delta\boldsymbol{B}_w)\right], \tag{15}$$

$$\frac{dz}{dt} = v_\parallel, \tag{16}$$

where $\boldsymbol{v}$ is the electron velocity, $B_0\boldsymbol{i}_z$ is the ambient magnetic field, and $\delta\boldsymbol{E}_w$ and $\delta\boldsymbol{B}_w$ are the wave magnetic field and electric field, respectively. The equations are solved with the Boris algorithm, and the time step $\Delta t = 0.01836\Omega_e^{-1}$. Initially the electrons are evenly distributed in a region with the length $512v_A/\Omega_i$, and the total number of electrons is 25,600.

The Alfvén waves are assumed to be intrinsic, and they propagate along the ambient magnetic filed in the +*z*-direction with a power spectrum. The wave magnetic field, $\delta\boldsymbol{B}_w(z, t)$, can be described as follows:

$$\delta\boldsymbol{B}_w = \sum_{j=1}^{N} B_j(\boldsymbol{i}_x \sin\phi_j + \boldsymbol{i}_y \cos\phi_j), \tag{17}$$

$$\phi_j = \omega_j t - k_j z + \varphi_j, \tag{18}$$

where φ_j is a phase constant and N is the number of modes. The frequency ω_j and wavenumber k_j satisfy the dispersion relation of the Alfvén waves,

$$k_j v_A = \frac{\omega_j}{\sqrt{1 - (\omega_j/\Omega_i)^2}}. \tag{19}$$

The electric field $\delta\boldsymbol{E}_w(z, t)$ is given as

$$\boldsymbol{E}_w = -\sum_{j=1}^{N} B_j \frac{\omega_j}{ck_j} \boldsymbol{i}_z \times (\boldsymbol{i}_x \sin\phi_j + \boldsymbol{i}_y \cos\phi_j), \tag{20}$$

where $\omega_j = \omega_1 + (j-1)\Delta\omega$, $\Delta\omega = (\omega_N - \omega_1)/(N-1)$. The mode amplitude $B_j/B_1 = (\omega_j/\omega_1)^{-q/2}$, and the value of q is taken to be 5/3. This means that the power spectrum of the Alfvén waves has index 5/3, which is the same as the generally accepted value in the solar wind (e.g., Villante 1980; Bavassano & Smith 1986; Marsch 1999; Ofman et al. 2002; Xie et al. 2004). The range of ω_j is between $0.1\Omega_p$ and $0.3\Omega_p$, and $N = 100$. In this frequency

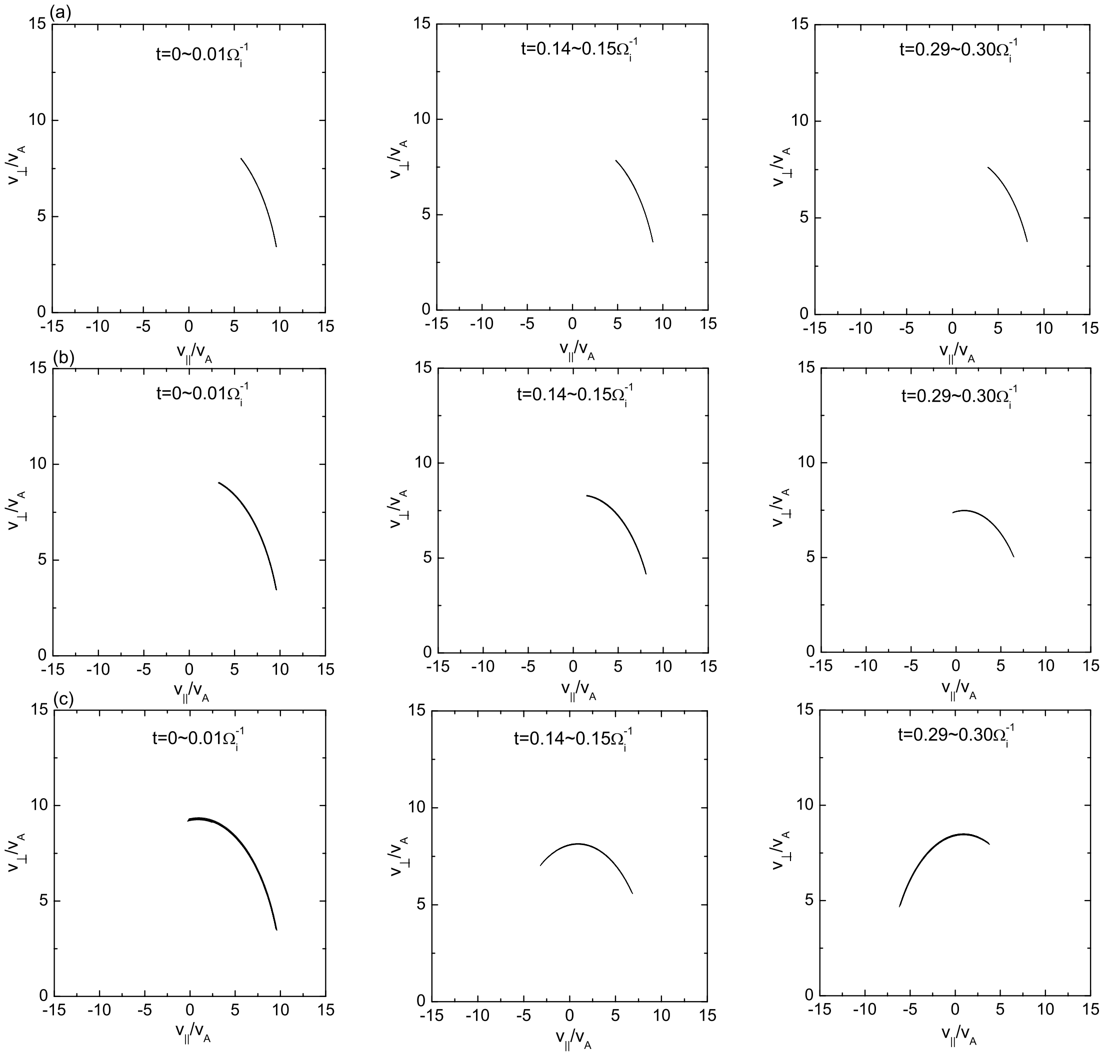

FIG. 5.—Typical electron trajectories in $v_\parallel - v_\perp$ coordinates during time periods $t = \sim 0{-}0.01\Omega_p^{-1}$, $\sim(0.14{-}0.15)\Omega_p^{-1}$, and $\sim(0.29{-}0.30)\Omega_p^{-1}$ for three cases: (*a*) $\delta B_w^2/B_0^2 = 0.064$, (*b*) $\delta B_w^2/B_0^2 = 0.142$, and (*c*) $\delta B_w^2/B_0^2 = 0.319$. The results are based on test particle calculations.

range, the electrons cannot rely on the resonance condition to interact with the Alfvén waves. What we are interested in this paper is the nonresonant interaction between the electrons and the finite-amplitude Alfvén waves. Three cases are considered in this paper, namely, (*a*) $\delta B_w^2/B_0^2 = 0.064$, (*b*) $\delta B_w^2/B_0^2 = 0.142$, and (*c*) $\delta B_w^2/B_0^2 = 0.319$.

Figure 3 shows the time evolution of the effective parallel temperature $T_\parallel/T_0$ and perpendicular temperature $T_\perp/T_0$ of the beam electrons for cases (*a*), (*b*), and (*c*), where T_0 is the initial effective temperature of the beam electrons. The subsequent effective temperature is calculated with the following procedure: the computational domain is evenly divided into 256 cells, and we first calculate the effective temperature in each cell; the effective temperature shown in the figure is the average value of the 256 cells. From the figure, we see that obviously the beam electrons are heated via nonresonant pitch-angle scattering. The heating is more effective in the direction perpendicular to ambient magnetic field than in the parallel direction. While the amplitude of the wave field is increased, the beam electrons are heated more effectively. Evidently the heating process does not rely on cyclotron resonance.

Figure 4 presents contour plots of the velocity distribution function of the beam electrons at different times for cases (*a*), (*b*), and (*c*). Initially, the velocity distributions of the beam electrons satisfy drift Maxwellian function with a drift speed equal to $15v_A$. In case (*a*) the beam electrons are pitch-angle scattered into a crescent shape at an initial stage. The other two cases show that as the amplitude of the wave fields increases, more and more electrons are scattered by the enhanced wave fields into velocity space where the electrons have negative $v_\parallel$. When the amplitude of the wave field becomes large, as in case (*c*), a nearly isotropic velocity distribution of the beam electrons is finally formed. The physics of this process can be easily understood through Figure 5, which depicts a typical electron trajectory in the $v_\parallel - v_\perp$ space at different times for the three cases: (*a*), (*b*), and (*c*). In these cases, the electron is supposed to have the same initial positions and velocities. When the amplitude of the enhanced wave field is increased, the range of the electron pitch angles also increases. This result is consistent with the theoretical analysis presented in § 2. However, in the test particle calculations, the dispersion relation of the frequency spectrum of the Alfvén waves satisfies equation (19), which is generalized and slightly different from the theoretical model. Therefore, the motion of the electron is not confined in the spherical surface that is described by equation (14). For case (*a*), the motion of the electron is confined in the right-hand part in $v_\parallel - v_\perp$ coordinates, while for case (*c*), the

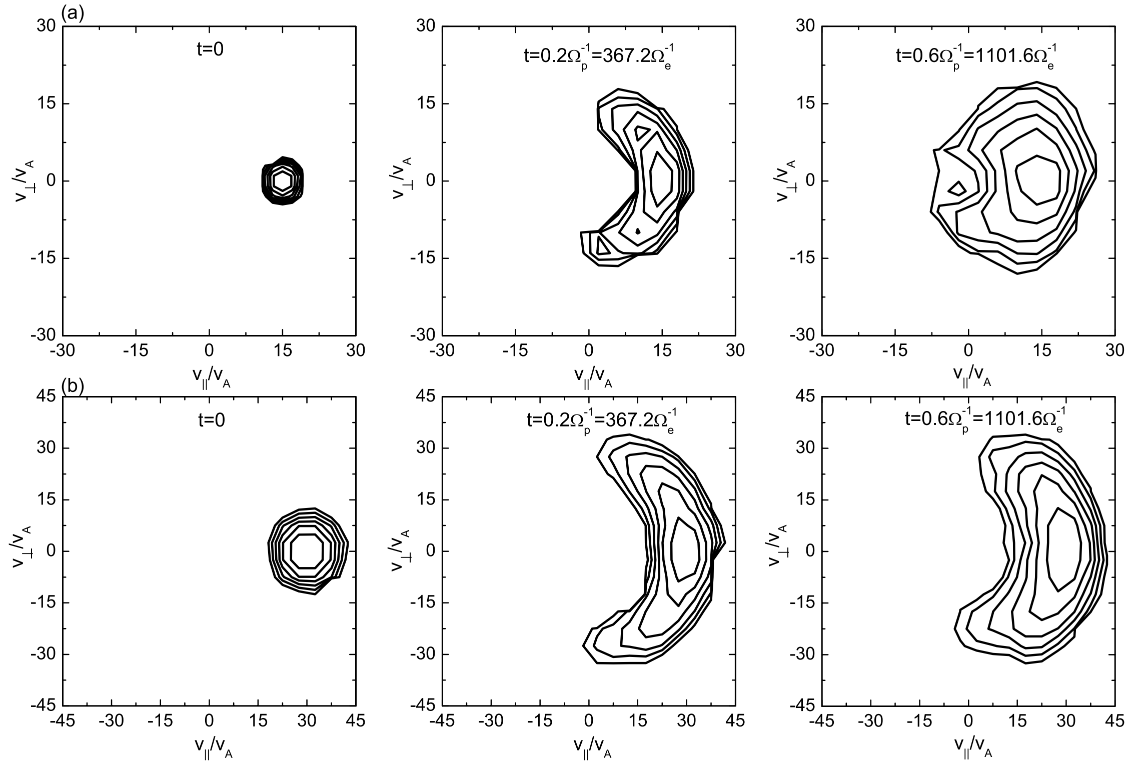

Fig. 6.—Contour plots of the velocity distribution function of the electron beam at $t = 0, 0.2\Omega_p^{-1}$, and $0.6\Omega_p^{-1}$ for two cases: (*a*) $v_{\rm the} = 1.0v_{\rm A}$, $u_b = 15v_{\rm A}$ and (*b*) $v_{\rm the} = 3.0v_{\rm A}$, $u_b = 30v_{\rm A}$, while keeping $\delta B_w^2/B_0^2 = 0.319$, where $v_\perp = (v_x^2 + v_y^2)^{1/2}$. The top half corresponds to $v_y > 0$, while the bottom half corresponds to $v_y < 0$. The contours represent logarithmically spaced levels. The results are based on test particle calculations.

electron can move to the left-hand part. Qualitatively we see that a nearly isotropic velocity distribution of the beam electrons may result when the amplitude of the wave field is sufficiently large.

We also change the parameters of the beam electrons to study their effect on the evolution of their distribution function, while keeping the amplitude of the Alfvén waves as $\delta B_w^2/B_0^2 = 0.319$. Figure 6 shows contour plots of the velocity distribution function of the beam electrons at different times. Compared with case (*c*), in Figure 6*a* the velocity dispersion is changed to $v_{\rm the} = 1.0v_{\rm A}$, and in Figure 6*b* the bulk velocity of the beam electrons is $u_b = 30v_{\rm A}$. Obviously, both cases show strong signs of scattering, and a nearly isotropic distribution is formed at the final stage in Figure 6*a*, which means that the final distribution of the beam electrons is insensitive to their initial velocity dispersion. And when the bulk velocity of the beam electrons is sufficiently large, a nearly isotropic distribution cannot be formed.

4. FURTHER DISCUSSION OF THE PHYSICAL PROCESS

In §§ 2 and 3 we present analytic and numerical studies of the scattering of a beam of energetic electrons by nonresonant interactions with intrinsic Alfvén waves. In this section we summarize and discuss the essence of the "scattering" process using a simple and basic explanation.

First of all, let us consider fast electrons moving along an ambient magnetic field such that initially they do not have perpendicular velocity. It is easily seen that these electrons would interact with the Alfvén-wave magnetic field, which is in the transverse direction. As a result of the $\boldsymbol{v} \times \delta\boldsymbol{B}_w$ force, these electrons are accelerated in the transverse direction. If the initial velocity of an electron is v_z, then the acceleration of this electron is proportional to $(v_z - v_A)\delta B_w$. Such a process is depicted by equation (7). Then from equation (8) we conceive that, in turn, an acceleration in the direction parallel to the ambient magnetic field would take place due to the force $\boldsymbol{v}_\perp \times \delta\boldsymbol{B}_w$. The results are displayed in expressions (10) and (11). An important point is that if the electron has a velocity v_z lower than the Alfvén waves, the waves tend to accelerate the electron. Otherwise the waves tend to decelerate the electrons. If initially the perpendicular velocity is very small and v_z is much higher than the Alfvén speed, the acceleration process is described by equation (13). As time goes on, $v_\perp$ may become progressively higher so that it is no longer negligible in equation (11). It is by this process the fast electrons are "scattered" by the Alfvén waves. At this point, we must reiterate that the solutions presented in equations (10) and (11) are obtained for very small $\delta B_w/B_0$. If $\delta B_w/B_0$ is finite but not very small, the test electron calculation discussed in § 4 should be more reliable than the analytic result. However, the basic physics is similar.

Finally we remark two salient points: (1) the scattering process discussed in this paper is effective for fast electrons, which have v_z much higher than the phase speed of Alfvén waves, and (2) it is a nonresonant wave-particle interaction process. The scattering process is different from the mirror scattering, which has been studied previously (Klimas & Sandri 1971, 1973; Fisk et al. 1974). The mirror scattering requires sufficiently large initial pitch angles, whereas the scattering process discussed in the present paper can occur even if the electron has zero initial pitch angle.

5. SUMMARY AND CONCLUSIONS

The primary purpose of the present paper is to show that intrinsic Alfvén waves can pitch-angle scatter fast electrons streaming along the ambient magnetic field so that eventually the electrons form a nearly isotropic distribution function, a result seen by in situ observations with *Wind* and other spacecraft. Such a scattering process does not rely on the cyclotron resonance process, which cannot take place between electrons and Alfvén waves, as is well known from linearized kinetic theories discussed in plasma physics. To demonstrate this point we have carried out both an analytic study and numerical calculations. Three conclusions are obtained: (1) Nonresonant interactions between Alfvén waves and electrons can be as effective as those between Alfvén waves and protons. (2) When the amplitude of the wave field is sufficiently large, the distribution function of a fast beam may be scattered into a nearly isotropic distribution. (3) Although the eventual distribution function looks stationary, the microscopic motion of each electron is not. In fact, each electron executes rapid oscillatory motion in the direction of its pitch angle. All these points are demonstrated in our discussion. These results are also consistent with the in situ observations: the beam electrons in almost all events show some signs of scattering (Krucker & Lin 2000; Maia et al. 2001; Haggerty & Roelof 2002; Simnett et al. 2002) or even form a nearly isotropic distribution function (Ergun et al. 1998). Point (3) also enables us to explain the physical meaning of the portion of the distribution function in which electrons have velocities in the sunward direction. Finally, we emphasize that in our numerical discussion the nearly isotropic distribution still exhibits a trace of a beam, just like the observational result displayed in Figure 1. The readers should not get the impression that the beam feature disappears completely in our scenario.

In conclusion, the most important point made in the present paper is that finite-amplitude Alfvén waves do interact with electrons via nonresonant interaction, a process that deserves our attention.

This research was supported by the National Science Foundation of China (NSFC) under grants 40336052 and 40304012, and Chinese Academy of Sciences grant KZCX3-SW-144.

REFERENCES

Akimoto, K., Winske, D., Gary, S. P., & Thomsen, M. F. 1993, J. Geophys. Res., 98, 1419
Bavassano, B., & Smith, E. J. 1986, J. Geophys. Res., 91, 1706
Belcher, J. W. 1971, ApJ, 168, 509
Chen, L., Lin, Z., & White, R. 2001, Phys. Plasmas, 8, 4713
Daughton, W., Gary, S. P., & Winske, D. 1999, J. Geophys. Res., 104, 4657
Ergun, R. E., et al. 1998, ApJ, 503, 435
Fisk, L. A., Goldstein, M. L., Klimas, A. J., & Sandri, G. 1974, ApJ, 190, 417
Grognard, R. J.-M. 1985, in Solar Radiophysics, ed. D. J. McLean & N. R. Labrum (Cambridge: Cambridge Univ. Press), 253
Haggerty, D. K., & Roelof, E. C. 2002, ApJ, 579, 841
Jacques, S. A. 1977, ApJ, 215, 942
Klimas, A. J., & Sandri, G. 1971, ApJ, 169, 41
———. 1973, ApJ, 180, 937
Krucker, S. K., & Lin, R. P. 2000, ApJ, 542, L61
Li, Y., Yoon, P. H., Wu, C. S., Weatherwax, A. T., Chao, J. K., & Wu, B. H. 1997, Phys. Plasmas, 4, 4103
Lin, R. P., Levedahl, W. K., Lotko, W., Gurnett, D. A., & Scarf, F. L. 1986, ApJ, 308, 954
Lin, R. P., Potter, D. W., Gurnett, D. A., & Scarf, F. L. 1981, ApJ, 251, 364
Lin, R. P., et al. 1995, Space Sci. Rev., 71, 125
———. 1996, Geophys. Res. Lett., 23, 1211
Maia, D., Pick, M., Hawkins, S. E., III, & Krucker, S. 2001, ApJ, 560, 1058
Marsch, E. 1999, Space Sci. Rev., 87, 1
Melrose, D. B., & Goldman, M. V. 1987, Sol. Phys., 107, 329
Muschietti, L. 1990, Sol. Phys., 130, 201
Ofman, L., & Davila, J. M. 1997, ApJ, 476, 357
Ofman, L., Gary, S. P., & Viñas, A. 2002, J. Geophys. Res., 107, SSH 9-1
Onsager, T. G., Winske, D., & Thomsen, M. F. 1991, J. Geophys. Res., 96, 1775
Pijpers, F. P. 1995, A&A, 295, 435
Simnett, G. M., Roelof, E. C., & Haggerty, D. K. 2002, ApJ, 579, 854
Tu, C. Y., & Marsch, E. 1997, Sol. Phys., 171, 363
Villante, U. 1980, J. Geophys. Res., 85, 6869
Winske, D., Wu, C. S., Li, Y. Y., Mou, Z. Z., & Guo, S. Y. 1985, J. Geophys. Res., 90, 2713
Wu, C. S., Yoon, P. H., & Chao, J. K. 1997, Phys. Plasmas, 4, 856
Xie, H., Ofman, L., & Viñas, A. 2004, J. Geophys. Res., 109, A08103
Yoon, P. H., & Wu, C. S. 1991, in Cometary Plasma Process, ed. A. D. Johnstone (Geophys. Monogr. 61; Washington: AGU), 241